Eur. Phys. J. E (2019) **42**: 120
DOI 10.1140/epje/i2019-11885-8

THE EUROPEAN PHYSICAL JOURNAL E

Regular Article

Deformation hysteresis of a water nano-droplet in an electric field

Fenhong Song[1], Dapeng Ju[1], Jing Fan[1], Qicheng Chen[1], and Qingzhen Yang[2,3,a]

[1] School of Energy and Power Engineering, Northeast Electric Power University, Jilin, Jilin 132012, P.R. China
[2] The Key Laboratory of Biomedical Information Engineering of Ministry of Education, School of Life Science and Technology, Xi'an Jiaotong University, Xi'an, Shaanxi 710049, P.R. China
[3] Bioinspired Engineering and Biomechanics Center (BEBC), Xi'an Jiaotong University, Xi'an, Shaanxi 710049, P.R. China

Received 31 March 2019 and Received in final form 28 May 2019
Published online: 10 September 2019
© EDP Sciences / Società Italiana di Fisica / Springer-Verlag GmbH Germany, part of Springer Nature, 2019

Abstract. Electric field is an effective method to manipulate droplets in micro/nano-scale, and various physical phenomena have been found due to the interaction of electric field and fluid flow. In this study, we developed a molecular dynamic model to investigate the deforming behavior of a nano-droplet in a uniform electric field. The nano-droplet was initially confined between two plates and then wetted on the lower plate (*i.e.*, substrate) until an equilibrium state, after that a uniform electric field in vertical direction was imposed to the system. Due to the electrical force, the droplet started to deform until achieving a new equilibrium state and the dynamic process is recorded. By comparing the equilibrium state under different electric field strength, we found a deformation hysteresis phenomenon, *i.e.*, different deformations were obtained when increasing and decreasing the electric field. To be specific, a large electric field ($E = 0.57\,\mathrm{V}\cdot\mathrm{nm}^{-1}$) is needed to stretch the nano-droplet to touch the upper plate, while a relatively lower field ($E = 0.40\,\mathrm{V}\cdot\mathrm{nm}^{-1}$) is adequate to keep it contacting with the plate. Accompanied by the deformation hysteresis, a distribution hysteresis of the average dipole orientations of water molecules in the nano-droplet is also found. Such a hysteresis phenomenon is caused by the electrohydrodynamic interactions between droplet and plates, and the findings of this study could enhance our understanding of droplet deformation in an electric field.

1 Introduction

Manipulating droplets has found wide-spreading applications in optoelectronic and microelectronic technologies, such as electrostatic spraying and painting [1,2], bioprinting [3], displaying devices [4], and micro/nano-manufacturing [5–8]. Among the numerous means, electric field is frequently adopted to manipulate and transport droplets due to its merits such as non-contact, good controllability and effectiveness in micro/nano scale. During these processes, a branching phenomenon might exist, *e.g.* two stable states of a droplet wetting on a fiber substrate in the presence of buoyancy was observed under the effect of an electric field [9]. In order to investigate the underlying mechanism, extensive work including both experimental and theoretical ones has been conducted to study the droplet deformation in an electric field.

In macroscopic systems, the famous Young-Lippmann equation listed as follows has been widely used to describe the dependence of the contact angle on the interfacial tensions and electric fields [10]:

$$\cos\theta = \frac{\gamma_{sg} - \gamma_{sl}}{\gamma_{lg}} + \frac{\langle \varepsilon\varepsilon_0 E \cdot E \rangle D}{2\gamma_{lg}}, \tag{1}$$

where θ represents the contact angle, γ the surface tension, ε the dielectric constant of the droplet, ε_0 the electric permittivity of free space, E the applied electric field strength and D the thickness of the interfacial double layer. The subscripts l, g and s refer to liquid, gas and solid, respectively. Some experiments have been conducted to investigate the static and dynamic electro-wetting of a macroscale droplet and found that the equilibrium contact angles obey the Young-Lippmann equation [11,12]. However, this equation fails to describe some phenomena in electro-wetting, for instance, the existence of a minimum saturation contact angle (*i.e.*, the droplet fails to spread to a film state) [13,14]. Another phenomenon is the contact angle hysteresis [15,16], and some researchers put forward an effective method to reduce the contact angle hysteresis by impregnating surfaces with a lubricant [17,18].

[a] e-mail: qzyang@mail.xjtu.edu.cn (corresponding author)

With the advances of micro/nano techniques, electro-wetting in micro/nano-scale has attracted considerable attention recently. When scaling down to micro-size or even nano-size, the wetting behaviors become different from that in the macroscale because of the significant effect of surface tension. For this case, the Young-Lippmann equation fails to describe the electro-wetting phenomena which assume the contact angle as a function of the electric field strength rather than the direction [10,19–21]. For a nano-scale droplet, the molecular dynamic simulation is a powerful tool. It can provide a deep insight from both structural and dynamic points of view into wetting and electro-wetting phenomena which are difficult to observe in experiments [22–26]. Molecular dynamic simulations have been used to study the static behaviors of a nano-droplet deforming on different substrates (*e.g.*, geometrically patterned substrates, substrate with molecular roughness, and flat substrate) under electric field [9,18,21,27]. Some interesting phenomena have been found, for instance, the nano-scale droplet might undergo a symmetrical or asymmetrical dynamic electro-wetting process, depending on the direction and strength of the electric field [19–21,28]. Ren *et al.* [25] investigated the effect of a uniform electric field on the interfacial structure and wetting properties of water droplets on a graphene solid substrate. The results showed that the average dipole moment of water molecules undergoes a noticeable disordered-to-ordered change, especially under the influence of an electric field $E \geq 0.80\,\mathrm{V}\cdot\mathrm{nm}^{-1}$. Zong *et al.* [29] found that the electric field direction has an obvious effect on the solid-liquid interfacial tension and the liquid-vapor interfacial tension exhibits a slight dependence on the electric field strength. In another molecular simulation study, the reported results by Kargara *et al.* [30] revealed that the nano-scale water droplet would be stretched along the electric field direction in a field stronger than $0.80\,\mathrm{V}\cdot\mathrm{nm}^{-1}$, while, the shape of a droplet will not change in an alternating field with the frequency above a threshold value.

All these researches efforts focus on the effect of electric field polarity and direction, surface rough microstructure on the electro-deforming process of the nano-droplet deforming on the substrate, as well as the thorough analysis on the static contact angles and interfacial tensions. While, the dynamic deforming behaviors and molecular properties of a nano-droplet induced by an electric field still need to be studied, especially the reverse electro-deforming behaviors are keen to be well understood at the nanoscale. Thus, it is necessary to further study the deforming mechanism of a nano-droplet under the coupling effect of substrate and electric field to meet the requirements in the potential applications. In this work, the molecular dynamic simulation method is adopted to investigate the deformation of a nano-droplet under electric fields. Both the equilibrium and dynamic deforming behaviors are studied systematically, as well as the distribution of the molecular dipole moment to reveal the effect of electric fields and solid substrates. It is found that a deformation hysteresis occurs when an electric field is increased and decreased, and the deforming path depends greatly on the field strength.

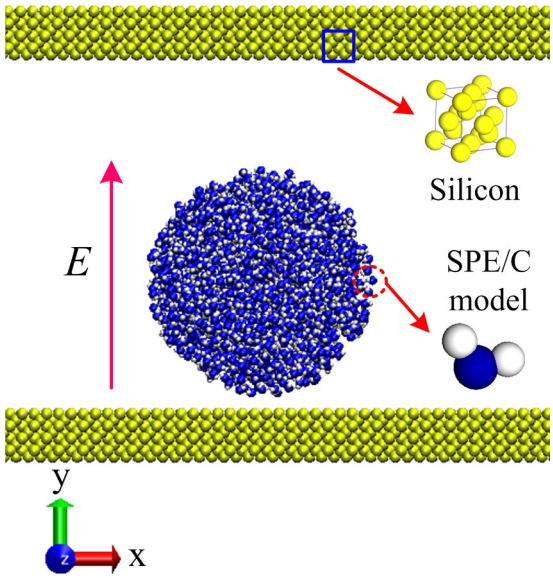

Fig. 1. The initial structure of water droplet and solid plates in the molecular simulation model.

2 Molecular simulation model

Figure 1 illustrates the initial structure of a nano-droplet and plates in the molecular simulation model. As shown, two solid plates spaced 7.0 nm apart are composed of 21632 silicon atoms arranged in a diamond lattice, with a lattice constant of 0.543 nm. To speed up the calculations, silicon atoms are kept frozen during all the molecular dynamic simulations, as often applied in the previous literature [10,19,20,28]. A nano-droplet composed of 2000 water molecules was initially established to a spherical one with a radius of about 2.2 nm. The simple point charge/extension (SPC/E) model is applied to the water molecule, for which the intermolecular interactions among water molecules are calculated as follows. The short-range van der Waals forces are calculated using the classical Lennard-Jones (12-6 L-J) potential, while the long-range electrostatic interactions applying Coulomb's law,

$$\phi(r_{ij}) = 4\varepsilon_{oo}\left[\left(\frac{\sigma_{oo}}{r_{oo}}\right)^{12} - \left(\frac{\sigma_{oo}}{r_{oo}}\right)^{6}\right] + \frac{1}{4\pi\varepsilon_0}\sum_{i=1}^{3}\sum_{j=1}^{3}\frac{q_i q_j}{r_{ij}} \tag{2}$$

where the first L-J potential term is only to calculate oxygen-oxygen interactions because the hydrogen atoms are too light and the interaction could be omitted. The second term is used to calculate the Coulomb force between the charged atoms, where q_i, q_j is the charge of the atom i, j, r_{ij} is the distance between atoms i and j, and ε_0 is the vacuum dielectric constant.

The intermolecular interactions between water molecules and silicon atoms are calculated by the modified L-J potential function

$$\phi_{ls}(r_{ij}) = 4\varepsilon_{ls}\left[\left(\frac{\sigma_{ls}}{r_{ij}}\right)^{12} - \left(\frac{\sigma_{ls}}{r_{ij}}\right)^{6}\right], \tag{3}$$

Table 1. Parameters of the atoms for the potential function.

Atom	σ (nm)	ε (kJ/mol)	q (e)
O	0.316	0.6502	−0.8476
H	0	0	0.4238
Si	0.3615	1.26	0.0

where σ_{ls} and ε_{ls} are obtained according to the Lorentz-Berthelot mixing rule [31]

$$\varepsilon_{ls} = \sqrt{\varepsilon_l} \cdot \varepsilon_s, \qquad \sigma_{ls} = (\sigma_l + \sigma_s)/2.0. \tag{4}$$

All the potential parameters and the charges for each type of atoms are listed in table 1. In order to ensure the solid surface was in hydrophobic, the potential parameter ε_{ls} between oxygen and silicon atom was reduced by half.

A smooth cut-off of 1.5 nm is applied for the short-range van der Waals forces' calculation and the Particle-Particle Particle-Mesh (PPPM) method is used to modify the long-range electrostatic interaction between atoms. When an external electric field E is imposed, an additional term indicating the electric field forces $f_{ie} = E \cdot q_i$ is applied on each atom depending on its charge q_i. All the molecular dynamic simulations are carried out using the LAMMPS soft package in the NVT ensemble [32]. The initial velocities of atoms are assigned randomly according to the temperature of the system. The Velocity-Verlet algorithm is employed to solve the Newtonian motion equations for each atom with a time step of 1 fs. The Nosé-Hoover thermostat [33] was applied at each time step to keep the simulation system at a desired temperature of 300 K. Firstly, the droplet deforming on the lower substrate was equilibrated in the absence of the electric field. Then a vertical electric field E_{y+} is applied to the system to investigate the deformation and wetting behaviors of a water nano-droplet.

3 Results and discussion

Employing the above molecular dynamic model, the deformation process of nano-droplet can be obtained. Once the electric field is imposed, the water molecules would change their attitude which can be denoted by the direction of the dipole moment. Due to the interaction of the electric field and the dipole moment (*i.e.*, electrical force), the droplet would keep evolving until reaching its equilibrium state. In this study, a special interest is given to the equilibrium state, dynamic process and dipole moment of water molecules under different electric field strength. To quantitively characterize the deformation, the height of the water droplet is chosen as the key parameter and monitored during the process. In the following sections, the equilibrium state, dynamic process and dipole moment under different electric field strength is studied and analyzed.

3.1 Equilibrium state of water droplet under electric field

The equilibrium state represents the final shape that a droplet eventually deforms into. We have studied the equilibrium state of water droplet under different electric field strength and the obtained results are illustrated in fig. 2. Without electric field ($E = 0\,\mathrm{V \cdot nm^{-1}}$), the nano-droplet tends to wet the substrate and its equilibrium state is a spherical cap. On this basis, the electric field is increased to $0.20\,\mathrm{V \cdot nm^{-1}}$ and the deformation has no obvious change since the electrical force is still small. When the electric field is increased to $0.45\,\mathrm{V \cdot nm^{-1}}$, one can see that the droplet is stretched longer in the vertical direction, *i.e.*, along the direction of electric field. It is worth noting that the present case is different from electro-wetting in which the droplet tends to spread along the horizontal direction when imposing an electric field. For electro-wetting the electric field is applied between droplet and substrate, and the strongest electric field appears at the contact line. Thus the droplet is stretched along the horizontal direction. In our case, however, the droplet is placed in an initially uniform electric field and the effect of the electric force is to stretch the droplet vertically along the direction of the electric field. Such a phenomenon is the same as the droplet deformation in macroscale which has been observed by other researchers [34–36].

If the electric field is further increased, the droplet deformation becomes more pronounced ($E = 0.50, 0.54, 0.56\,\mathrm{V \cdot nm^{-1}}$). When the electric field gets to $0.57\,\mathrm{V \cdot nm^{-1}}$, the droplet would deform dramatically until it gets in contact with the top plate and the corresponding equilibrium state in this case is a so-called "liquid bridge". For an even higher electric field $E = 0.60\,\mathrm{V \cdot nm^{-1}}$, the droplet keeps contacting the two plates with the "liquid bridge" equilibrium state. Actually the reason that we add the top plate is to provide a constraint for the droplet; otherwise the droplet will eventually be stretched to a single line and might break into breads under a strong enough electric field. Comparing the equilibrium deformations at $E = 0.56\,\mathrm{V \cdot nm^{-1}}$ and $0.57\,\mathrm{V \cdot nm^{-1}}$, one can see that a small increase of the electric field causes a remarkable difference of the droplet deformation. Such a value $E = 0.56\,\mathrm{V \cdot nm^{-1}}$ is defined as the critical electric field strength. The nano-droplet would keep evolving to contact the upper plate if the electric field is above this critical value. Eventually, the droplet "bridges" the two plates.

In fig. 2, the equilibrium state is obtained by increasing the electric field. For instance, in order to get the deformation at $E = 0.57\,\mathrm{V \cdot nm^{-1}}$, the shape at $E = 0.56\,\mathrm{V \cdot nm^{-1}}$ is chosen as the initial state. One may put forward a question that the equilibrium state may be different if the electric field is decreased from a higher value down to 0. Thus, we decreased the electric field and studied the droplet deformation, and the obtained results are exhibited in fig. 3. We started from $E = 0.60\,\mathrm{V \cdot nm^{-1}}$ as the first case. The equilibrium state is a "liquid bridge" which is the same as in the previous study. Then the electric field is decreased to $0.50\,\mathrm{V \cdot nm^{-1}}$, rather than falling

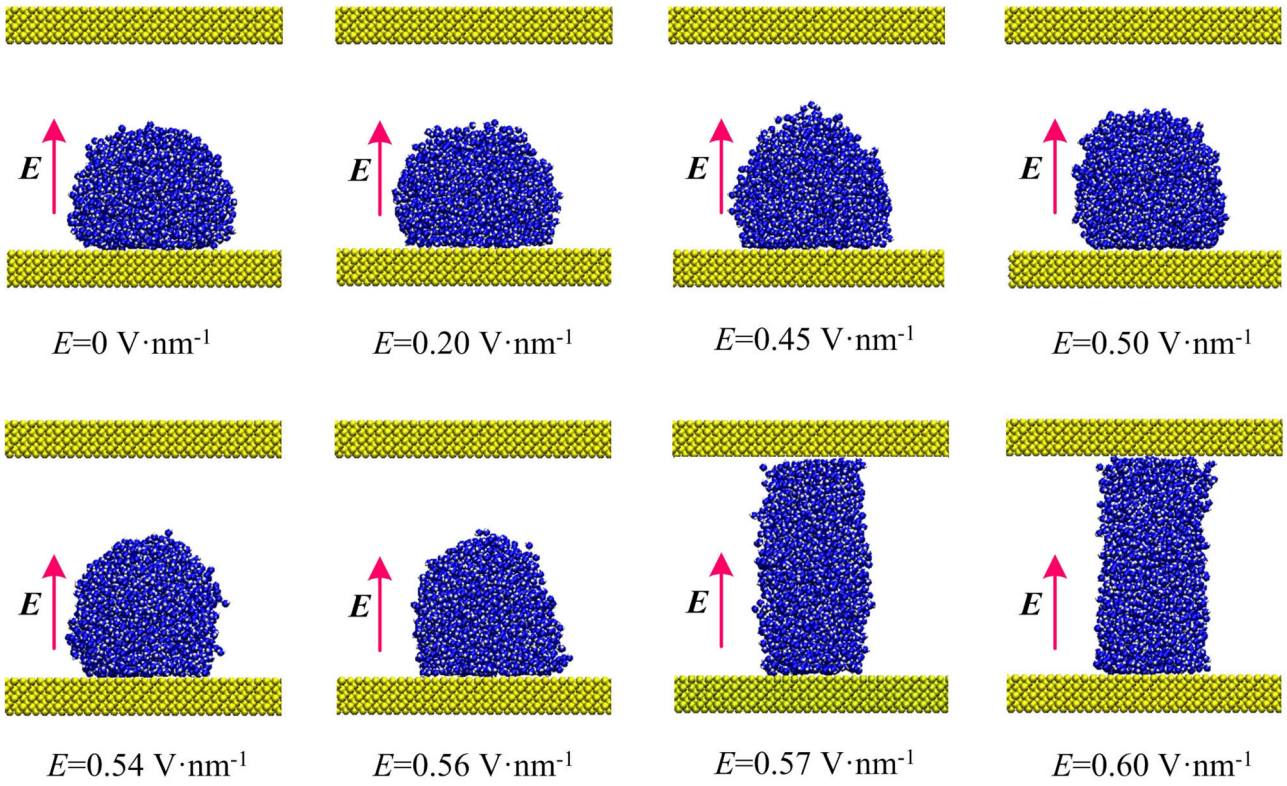

Fig. 2. Snapshots for the equilibrium state of a water droplet with the electric field increasing from 0 to $0.60\,\mathrm{V}\cdot\mathrm{nm}^{-1}$.

down the droplet still contacts with the top plate. This is different from the previous study in which the droplet does not contact the top plate for an electric field lower than $0.57\,\mathrm{V}\cdot\mathrm{nm}^{-1}$ (see fig. 2). If the electric field is further decreased ($E = 0.40\,\mathrm{V}\cdot\mathrm{nm}^{-1}$), the droplet would detach from the top plate. For an even lower electric field ($E = 0.38\,\mathrm{V}\cdot\mathrm{nm}^{-1}$), the droplet would recede back to a spherical cap. After that, there appears no obvious change in the droplet deformation when the electric field is further decreased down to 0.

To quantitatively characterize the deformation of the nano-droplet, the height (*i.e.*, from the bottom plate to the highest point of the droplet) is recorded during the deforming process. For each electric field, the height of the droplet at the equilibrium state can be obtained as an average value of the height in several equilibrium snapshots. The dependence of the height on the applied electric field E is plotted in fig. 4, and both "increasing" and "decreasing" cases are depicted for a comparison. One can see that the droplet height increases gradually if the electric field is increased from 0. When the electric field strength comes to the critical value, $E = 0.56\,\mathrm{V}\cdot\mathrm{nm}^{-1}$, a small increment of the electric field would cause a remarkable increase of the droplet deformation, *e.g.* when $E = 0.57\,\mathrm{V}\cdot\mathrm{nm}^{-1}$, the droplet has contacted with the top plate and the corresponding equilibrium state is a "liquid bridge". If the electric field is further increased, the nano-droplet would spread along the lower and upper plates. The height of the droplet however would remain the same.

After that, we start to decrease the electric field strength. It is surprising that the "decreasing" curve deviates from the "increasing" one (see fig. 4). As indicated by the "decreasing" curve, the droplet still "bridges" the two plates until the electric field is decreased down to $E = 0.40\,\mathrm{V}\cdot\mathrm{nm}^{-1}$. A further decrease of the electric field would cause the droplet to detach from the top plate. Such a value $E = 0.40\,\mathrm{V}\cdot\mathrm{nm}^{-1}$ can be defined as the second critical electric field strength. After that, the electric field is the equilibrium deformation which coincides with the "increasing" curve. Comparing the "increasing" and "decreasing" curves, one can notice a deformation hysteresis phenomenon. If the electric field strength is between the two critical values (*i.e.*, $E = 0.40\,\mathrm{V}\cdot\mathrm{nm}^{-1}$ and $E = 0.56\,\mathrm{V}\cdot\mathrm{nm}^{-1}$), two equilibrium states may exist and which one is taken depends on the electric field is increased or decreased to the present value. Such a hysteresis phenomenon is caused by the nonlinear interaction between the electric field and droplet deformation. Actually similar phenomena have been found in other nonlinear systems [37,38].

3.2 Dynamic deforming behaviors of a nano-droplet

In the previous section, the equilibrium state of a nano-droplet has been studied and it is found that the shape depends on the electric field strength. In the following, we would study the dynamic behaviors of droplet deformation and focus on the process of the droplet evolution to-

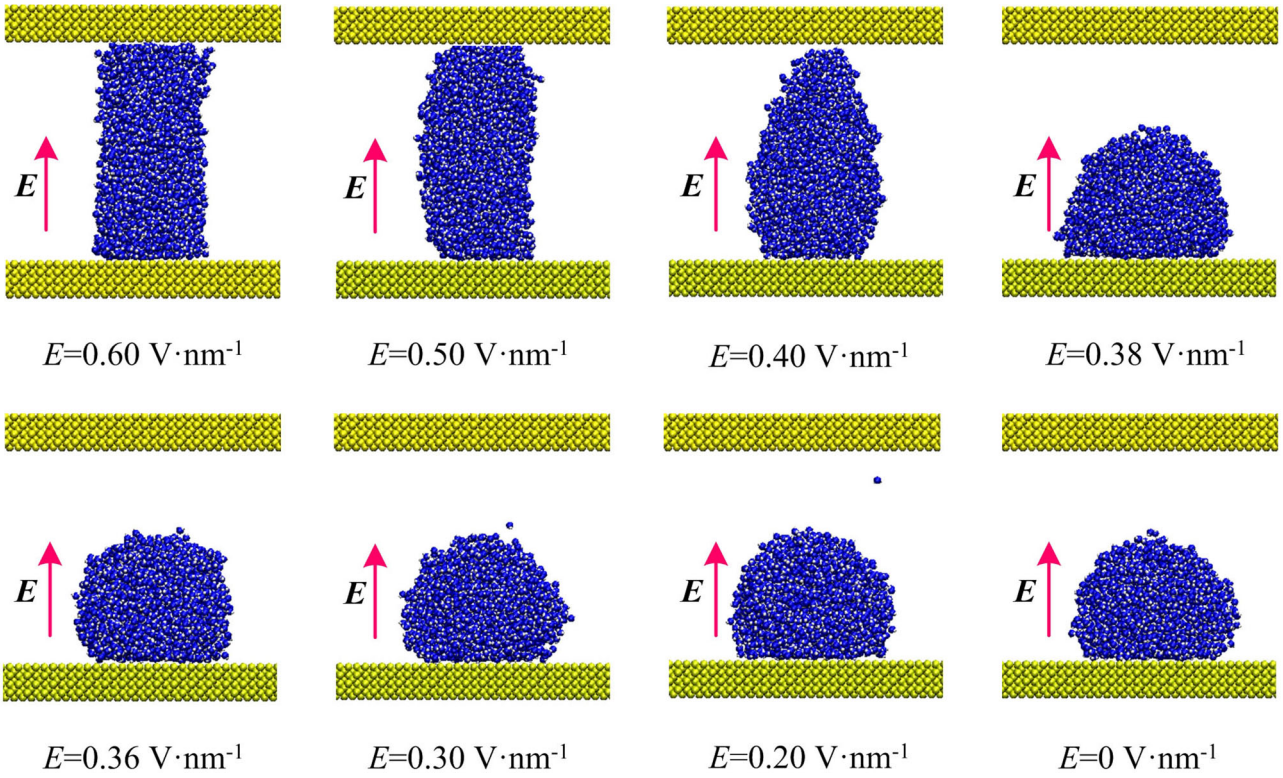

Fig. 3. Snapshots for the equilibrium state of a water droplet with the electric field decreasing from 0.60 to $0\,\mathrm{V}\cdot\mathrm{nm}^{-1}$.

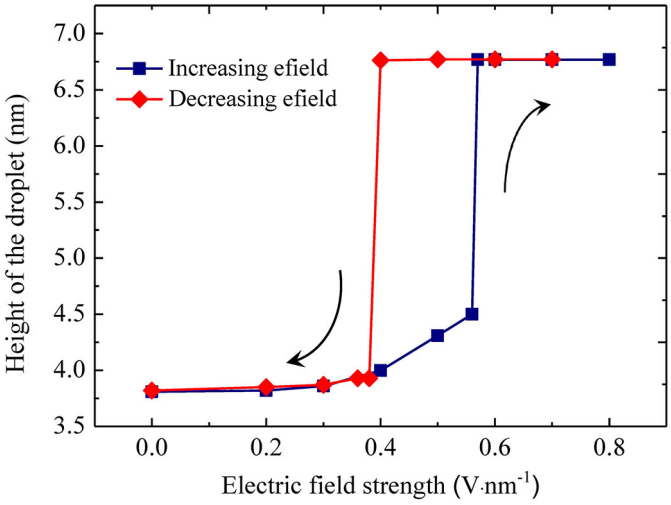

Fig. 4. The height of the water droplet with the increasing electric field from 0 to $0.60\,\mathrm{V}\cdot\mathrm{nm}^{-1}$ and the reverse process of the decreasing electric field from 0.60 to $0\,\mathrm{V}\cdot\mathrm{nm}^{-1}$.

wards its equilibrium state. When increasing the electric field, the critical value is $E_c = 0.56\,\mathrm{V}\cdot\mathrm{nm}^{-1}$. We chose two typical electric field strength ($E = 0.50\,\mathrm{V}\cdot\mathrm{nm}^{-1}$ and $E = 0.60\,\mathrm{V}\cdot\mathrm{nm}^{-1}$), one is lower that this value and the other higher than it. The droplet starts to deform from the initial state and the obtained results are depicted in fig. 5. To understand the deformation mechanisms, some snapshots at different time are chosen to reveal the transient deformation process in an electric field.

The initial state ($t = 0$) is chosen as the equilibrium deformation at $E = 0\,\mathrm{V}\cdot\mathrm{nm}^{-1}$. For the case of $E = 0.50\,\mathrm{V}\cdot\mathrm{nm}^{-1}$ (lower than the critical electric field strength), the nano-droplet deforms gradually ($t = 50\,\mathrm{ps}$) in the vertical direction due to the action of the electrical force. Comparing the droplet height at $t = 100\,\mathrm{ps}$ and $t = 500\,\mathrm{ps}$, one can see that the droplet achieves its equilibrium state after $t = 100\,\mathrm{ps}$ (see fig. 5(a)). The equilibrium shape is consistent with the previous study, *i.e.*, the equilibrium state is a slightly deformed spherical cap when the electric field is lower than the critical value. For an electric field $E = 0.60\,\mathrm{V}\cdot\mathrm{nm}^{-1}$ (higher than E_c), the droplet keeps growing in the vertical direction. At $t = 270\,\mathrm{ps}$, some molecules have arrived at the top plate. After that, more molecules get in contact with the top plate. At $t = 500\,\mathrm{ps}$, a "liquid bridge" forms. Comparing with the equilibrium state at $E = 0.60\,\mathrm{V}\cdot\mathrm{nm}^{-1}$ (see fig. 2), one can conclude that the droplet reaches its equilibrium at $t = 500\,\mathrm{ps}$.

During the deformation process, the droplet height is recorded and the evolution of the droplet height is plotted in fig. 6. When the electric field is lower than critical value $E_c = 0.56\,\mathrm{V}\cdot\mathrm{nm}^{-1}$, the droplet would deform gradually until achieving its equilibrium state (see the curves of $0.30\,\mathrm{V}\cdot\mathrm{nm}^{-1}$ and $0.50\,\mathrm{V}\cdot\mathrm{nm}^{-1}$). After that the droplet height would be fixed. The difference between $0.30\,\mathrm{V}\cdot\mathrm{nm}^{-1}$ and $0.50\,\mathrm{V}\cdot\mathrm{nm}^{-1}$ is that a higher electric field results in a faster growth rate and a larger deformation, *i.e.*, droplet height. For the electric field $E = 0.60\,\mathrm{V}\cdot\mathrm{nm}^{-1}$ which is larger than the critical value, the deformation process has gone through a few stages.

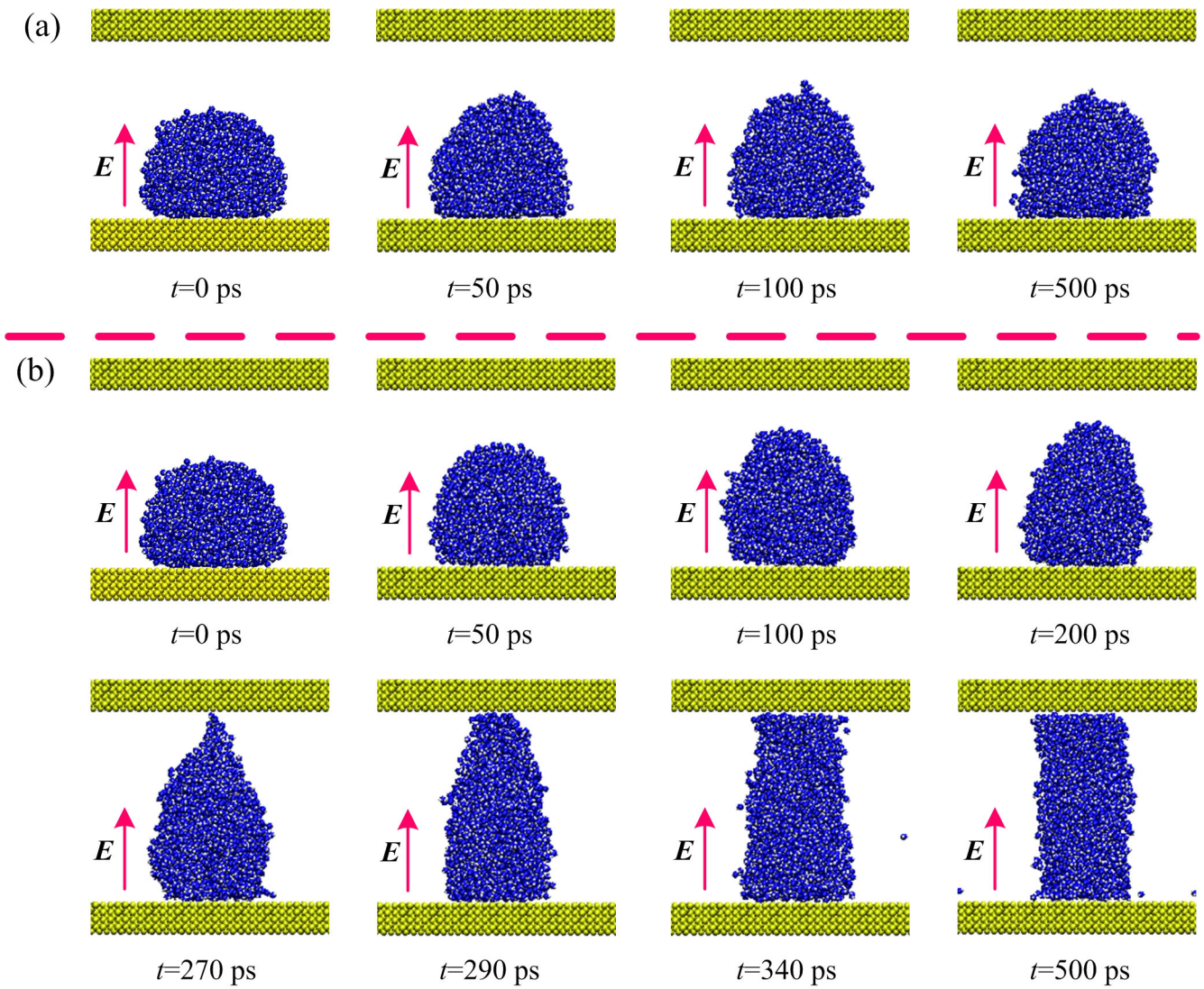

Fig. 5. The dynamic deforming process of a nano-droplet under electric field (a) $E = 0.50\,\mathrm{V}\cdot\mathrm{nm}^{-1}$ and (b) $E = 0.60\,\mathrm{V}\cdot\mathrm{nm}^{-1}$.

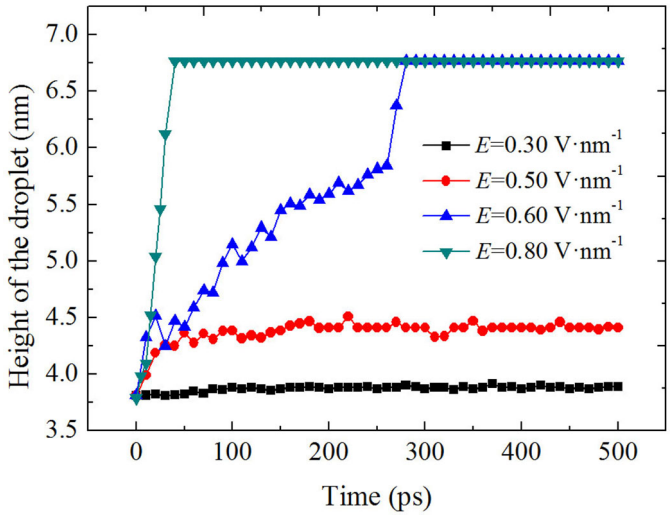

Fig. 6. Time evolution of the height of a nano-droplet under different electric fields.

At the beginning, the droplet deforms rapidly since the electrical force dominates the process and the surface tension is relatively small. With the increase of deformation, the effect of the surface tension becomes significant (the effect of the surface tension is proportional to the deformation) and is comparable to the electrical force. Due to the hindering effect, the droplet slowly deforms in a uniform manner (from $t = 50\,\mathrm{ps}$ to $260\,\mathrm{ps}$). With the increase of the droplet deformation, the distance between the droplet and the upper plate decreases and the molecular interaction between droplet and plate (LJ force) comes into play. The deformation of the droplet speeds up due to the attraction from upper plate. At time $t = 270\,\mathrm{ps}$, the water molecule starts to contact with the upper plate. Then more molecules spread on the upper plate and the contacting area becomes larger. Eventually an equilibrium liquid bridge is formed when the electric field forces are balanced by the interfacial interaction between the droplet and the plates. For comparison, an electric field $E = 0.80\,\mathrm{V}\cdot\mathrm{nm}^{-1}$ (much larger than E_c) is also studied.

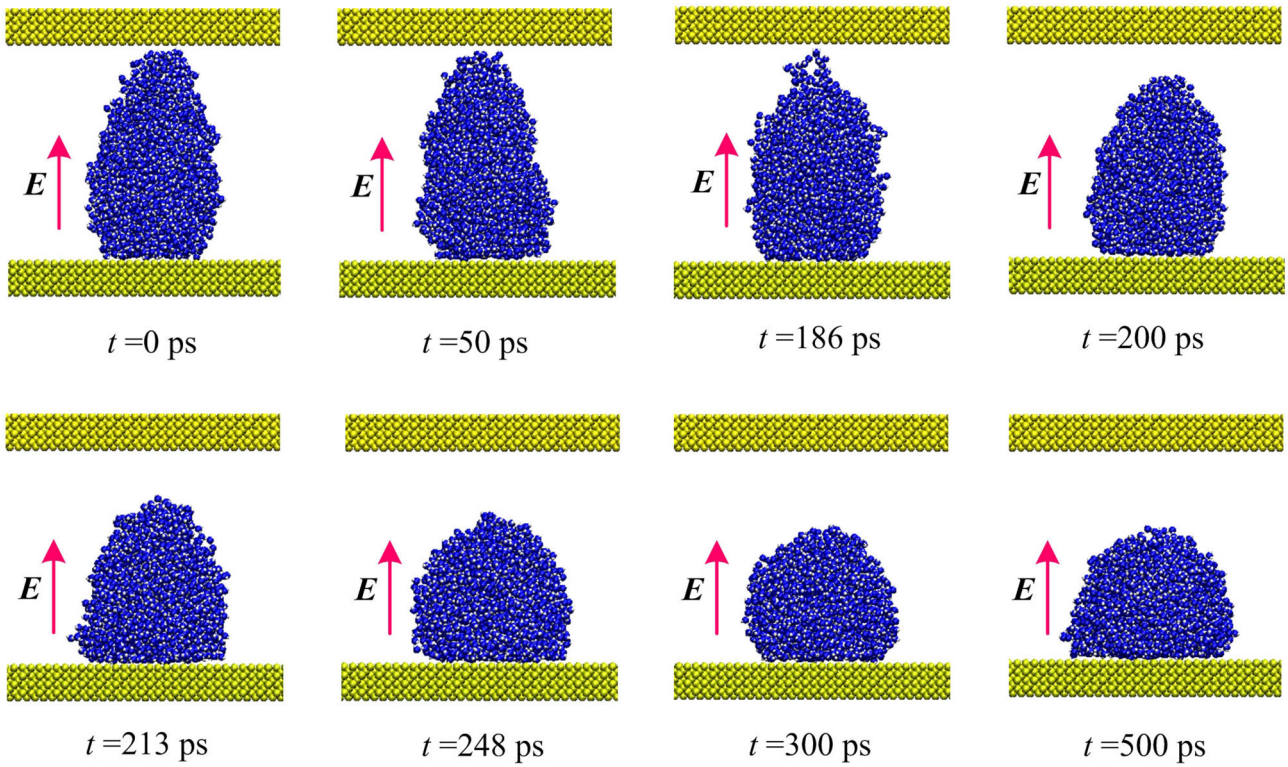

Fig. 7. Snapshots for the dynamic deformation of a water droplet while the electric field decreases from 0.40 to 0.38 $\mathrm{V \cdot nm^{-1}}$.

In this case, the electrical force is much larger than surface tension. Thus the droplet deforms dramatically and gets in contact with the upper plate at $t = 30$ ps. Then the droplet spreads along the upper plate until its equilibrium state.

3.3 Dynamic detaching process of a nano-droplet

In the above section, the dynamic process is obtained by increasing the electric field (the initial state is chosen as the equilibrium state at $E = 0\,\mathrm{V \cdot nm^{-1}}$). This process could be different if the electric field is decreased. In order to enhance our understanding of the deformation process, we would decrease the electric field and observe the process of droplet detaching from the upper plate. As discussed before, the nano-droplet will detach from the upper plate when the electric field strength is smaller than the second critical value $0.40\,\mathrm{V \cdot nm^{-1}}$. Thus we decrease the electric field strength from $0.40\,\mathrm{V \cdot nm^{-1}}$ to $0.38\,\mathrm{V \cdot nm^{-1}}$ and the snapshots of the droplet deformation are shown in fig. 7.

Once the electric field is decreased, the stretch force becomes smaller and is not sufficient to keep the droplet contacting with the upper plate. For the water molecules on top of the nano-droplet, the interactions from the nano-droplet becomes stronger than the absorption force from the upper plate, thus the molecules tend to move down and the nano-droplet detaches from the top plate ($t = 186$ ps). After that, the distance between the droplet and the upper plate is larger than the cutoff radius, the effect of the upper plate disappears and the droplet keeps deforming.

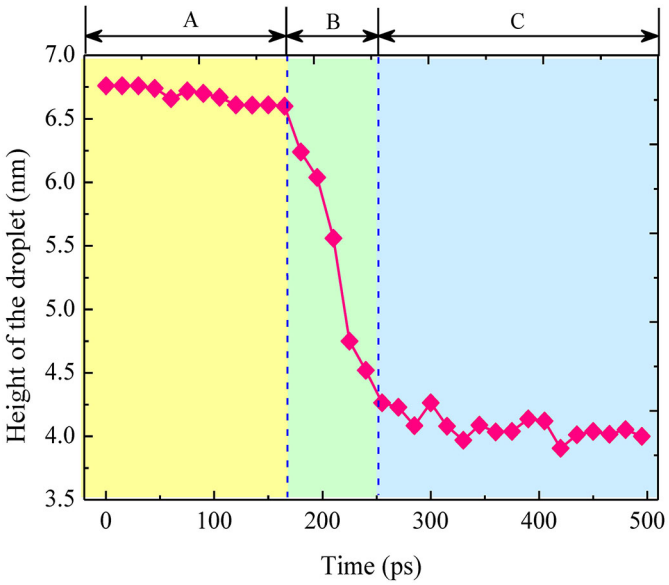

Fig. 8. Time evolution of the height of a nano-droplet while the electric field decreases from 0.40 to 0.38 $\mathrm{V \cdot nm^{-1}}$.

Eventually, the droplet achieves its equilibrium state, *i.e.*, a spherical cap.

During this dynamic process, the evolution of the nano-droplet height is monitored and plotted in fig. 8. For this case, the transient process undergoes three stages which have been marked as A, B and C for convenience. In stage A ($t < 165$ ps), the equilibrium state of the nano-droplet is broken after the electric field decreases from

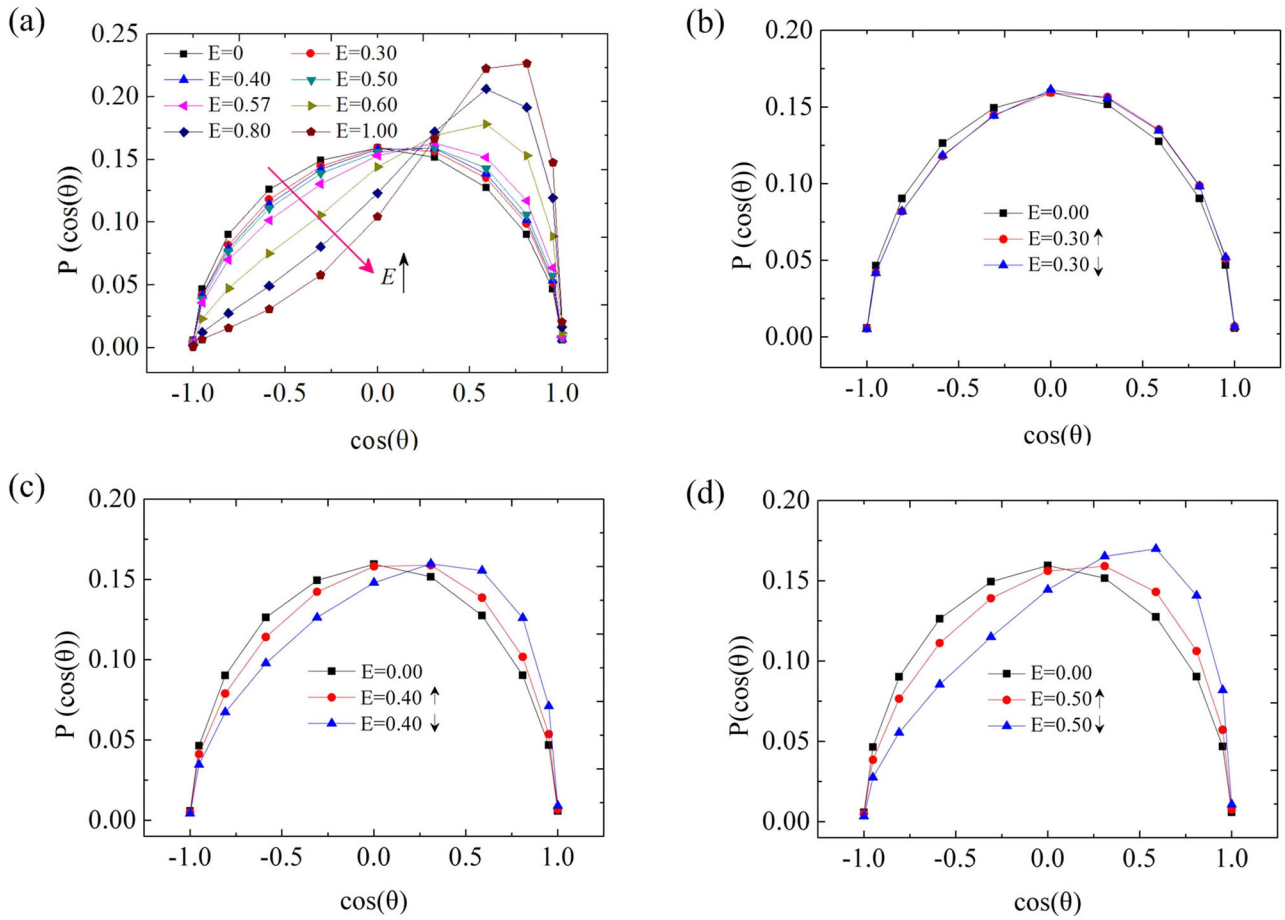

Fig. 9. Distribution of the average polarizations of water molecules in an electric field. (a) The electric field is increased from 0 to $1.0\,\mathrm{V}\cdot\mathrm{nm}^{-1}$; (b), (c) and (d) are the comparison between the increasing and the decreasing process in $E = 0.30\,\mathrm{V}\cdot\mathrm{nm}^{-1}$, $E = 0.40\,\mathrm{V}\cdot\mathrm{nm}^{-1}$ and $E = 0.50\,\mathrm{V}\cdot\mathrm{nm}^{-1}$. The symbol "↑" indicates the electric field is increased to this value and the symbol "↓" represents the decrease.

$0.4\,\mathrm{V}\cdot\mathrm{nm}^{-1}$ to $0.38\,\mathrm{V}\cdot\mathrm{nm}^{-1}$. The interaction between water molecules and top plate still exists which hinders the detaching process, thus the droplet height decreases slowly. In stage B ($165 < t < 300\,\mathrm{ps}$), the top of the droplet detaches from the upper plate, and the interactions between water molecules and top plate disappear. In this stage, the movement of the water molecule is dominated by the force with other water molecules and that with the lower plate. Thus the droplet deforms rapidly which can be indicated by the decreasing rate of the droplet height. To be specific, the height decreases from 6.5 nm to 4.2 nm. In stage C ($t > 300\,\mathrm{ps}$), the droplet is approaching its equilibrium state and the surface tension and electrical force can nearly balance each other. Thus the droplet height decreases in a slow manner. At the end ($t = 500\,\mathrm{ps}$), the droplet achieves its equilibrium state and the droplet height keeps constant.

3.4 Distribution of water molecular dipole moment

As a typical polar molecule, a water molecule tends to rearrange itself under the effect of an external electric field owning to the opposite electric field forces acting on hydrogen and oxygen atoms. Essentially, the deformation of the nano-droplet is determined by the movement of water molecules, and the molecules movement is governed by three competing forces including solid-liquid intermolecular forces, liquid-liquid intermolecular forces and the external electric field force. The polarization of water molecules would affect the electrical force. Thus in this section we would study the average polarization of water molecules in a different electric field.

Using the aforementioned molecular dynamic model, the equilibrium state of a nano-droplet in an electric field can be obtained. For each equilibrium state, the average polarization of water molecules along the electric field direction is analyzed. Figure 9 shows the statistical results when electric field increases from 0 to $1.0\,\mathrm{V}\cdot\mathrm{nm}^{-1}$. The symbol θ represents the angle between the water molecular dipole moment vector and the electric field direction ($y+$), and P denotes the percentage. As revealed in the figure, the direction of water molecules is random and disordered when $E = 0\,\mathrm{V}\cdot\mathrm{nm}^{-1}$. The profile shows a symmetric and broad orientation distribution. With the increase of the electric field, water molecules tend to rotate themselves with hydrogen atoms directing to the electric field and the oxygen atom in the opposite direction. The dipole moment shows a slight change at weak electric fields because the

restrain forces from other water molecules are hindering such a movement. As stated before, if the electric field is higher than the critical value $E = 0.56\,\mathrm{V}\cdot\mathrm{nm}^{-1}$, the nano-droplet would contact the upper plate and the interfacial interaction with the upper plate also contribute to the movement of water molecules. As indicated by the curve $E = 0.60\,\mathrm{V}\cdot\mathrm{nm}^{-1}$, the dipole moment changes obviously, *i.e.*, the molecules rotate themselves and comply with the direction of electric field. With the electric field further increase, more water molecular dipoles exhibit an obvious orientation parallel to the electric field direction because the external applied electric field force is strong enough to dominate the rearrangement of water molecules.

In the previous section, it has been found that the equilibrium state of a nano-droplet depends on the electric field strength and the way to impose the field (increase or decrease). A hypothesis is put forward that the molecular dipole moment could be different if the electric field is decreased to the value. Firstly, we chose the electric field as $E = 0.30\,\mathrm{V}\cdot\mathrm{nm}^{-1}$ which is lower than the critical value. For this case, the distribution of the water molecular dipole moment is almost the same in both paths because their equilibrium states are the same with the same droplet height (see fig. 9(b)). If the electric field strength is between the first critical value ($E = 0.56\,\mathrm{V}\cdot\mathrm{nm}^{-1}$) and the second critical value ($E = 0.40\,\mathrm{V}\cdot\mathrm{nm}^{-1}$), two equilibrium states could be obtained depending on the electric field is increased to such a value or decreased to it.

Take $E = 0.40$ and $0.50\,\mathrm{V}\cdot\mathrm{nm}^{-1}$ for instance, if electric field is decreased to this value more water molecules would follow the direction of the electric field (see figs. 9(c) and 9(d)).

4 Conclusions

In this paper we have developed a molecular dynamic model to investigate the equilibrium and transient deformation of a nano-droplet in an electric field. The external applied electric field would realign the water molecular dipoles and impose the electrical force upon them, and thus affect the deforming behaviors of the nano-droplet. It is found that the droplet deformation increases with the electric field and the droplet would get in contact with the top plate when the electric field gets to be a little higher than a critical value $E = 0.56\,\mathrm{V}\cdot\mathrm{nm}^{-1}$. Once the droplet contacts the top plate, a relatively lower electric field ($E = 0.40\,\mathrm{V}\cdot\mathrm{nm}^{-1}$) is sufficient to maintain it contacting with the plate. Thus a hysteresis phenomenon is found, two equilibrium states may exist when $0.40 \leq E \leq 0.56\,\mathrm{V}\cdot\mathrm{nm}^{-1}$. The dynamic deforming process reveals that nano-droplet deforming undergoes different paths depending on the electric field strength. Moreover, we studied the dipole moment of water molecules in an electric field and found that the dipole moment also depends on how the electric field is applied, *i.e.*, increased to this value or decreased. The findings in this paper may enhance our understanding of the deformation behaviors of a nano-droplet in an electric field.

The authors would like to acknowledge the support from the National Natural Science Foundation of China (Grant Nos. 51606032, 51605377), Jilin Province Science and Technology Project (Grant No. 20190103065JH).

Author contribution statement

Fenhong Song, Jing Fan and Qingzhen Yang conceived and designed the simulations; Dapeng Ju and Qicheng Chen performed the simulations and analyzed the data; Fenhong Song and Qingzhen Yang wrote the paper.

Publisher's Note The EPJ Publishers remain neutral with regard to jurisdictional claims in published maps and institutional affiliations.

References

1. B.K. Ku, S.S. Kim, J. Electrostat. **57**, 109 (2003).
2. M. Barlettaa, A. Gisario, Prog. Org. Coat. **64**, 339 (2009).
3. B. Gao, Q. Yang, X. Zhao, G. Jin, Y. Ma, F. Xu, Trends Biotechnol. **34**, 746 (2016).
4. H. You, A.J. Steckl, Appl. Phys. Lett. **97**, 023514 (2010).
5. X. Chen, X. Li, J. Shao, N. An, H. Tian, C. Wang, T. Han, L. Wang, B. Lu, Small **13**, 1604245 (2017).
6. E. Schaffer, T.T. Albrecht, T.P. Russell, U. Steiner, Lett. Nat. **403**, 874 (2000).
7. X.G. Liang, W. Zhang, M.T. Li, Q.F. Xia, W. Wu, H.X. Ge, X.Y. Huang, S.Y. Chou, Nano Lett. **5**, 527 (2005).
8. H. Tian, J. Shao, X. Chen, L. Wang, Y. Ding, J. Micromech. Microeng. **27**, 025008 (2017).
9. R. Ruiter, J. Ruiter, H.B. Eral, C. Semprebon, M. Brinkmann, F. Mugele, Langmuir **28**, 13300 (2012).
10. C.D. Daub, D. Bratko, K. Leung, A. Luzar, J. Phys. Chem. C **111**, 505 (2007).
11. S.R. Mahmoudi, K. Adamiak, G.S. Peter Castle, Proc. R. Soc. A **467**, 3257 (2011).
12. C. Decamps, J.D. Coninck, Langmuir **16**, 10150 (2000).
13. F. Mugele, J.C. Baret, J. Phys.: Condens. Matter **17**, R705 (2005).
14. F. Mugele, Soft Matter **5**, 3377 (2009).
15. R. Zhao, Q.C. Liu, P. Wang, Z.C. Liang, Chin. Phys. B **24**, 086801 (2015).
16. W.C. Nelson, P. Sen, C.J. Kim, Langmuir **27**, 10319 (2011).
17. E. Bormashenko, R. Pogreb, Y. Bormashenko, H. Aharoni, E. Shulzinger, R. Grinev, D. Rozenman, Z. Rozenman, RSC Adv. **5**, 32491 (2011).
18. Z. Brabcova, G. McHale, G.G. Wells, C.V. Brown, M.I. Newton, Appl. Phys. Lett. **110**, 121603 (2017).
19. C.D. Daub, D. Bratko, A. Luzar, Top Curr. Chem. **307**, 155 (2012).
20. F. Song, B. Li, C. Liu, Langmuir **29**, 4266 (2013).
21. T. Yen, Mol. Simul. **38**, 509 (2012).
22. F.H. Song, B.Q. Li, Y. Li, Phys. Chem. Chem. Phys. **17**, 5543 (2015).
23. Q. Li, Y. Xiao, X. Shi, S. Song, Nanomaterials **7**, 265 (2017).

24. D. Niu, G. Tang, Int. J. Heat Mass Transfer. **79**, 647 (2014).
25. H. Ren, L. Zhang, X. Li, Y. Li, W. Wu, H. Li, Phys. Chem. Chem. Phys. **17**, 23460 (2015).
26. J. Wang, S. Chen, D. Chen, Phys. Chem. Chem. Phys. **17**, 30533 (2015).
27. F. Song, L. Ma, J. Fan, Q. Chen, L. Zhang, B. Li, Nanomaterials **8**, 340 (2018).
28. F. Song, L. Ma, J. Fan, Q. Chen, G. Lei, B. Li, Phys. Chem. Chem. Phys. **20**, 11987 (2018).
29. D. Zong, Z. Yang, Y. Duan, Appl. Therm. Eng. **122**, 71 (2017).
30. M. Kargara, A. Lohrasebi, Phys. Chem. Chem. Phys. **19**, 26833 (2017).
31. M.P. Allen, D.J. Tildesley, J.R. Banavar, *Computer Simulation of Liquids* (Oxford University Press, New York, USA, 1989).
32. S. Plimpton, J. Comput. Phys. **117**, 1 (1995).
33. P.H. Hünenberger, Adv. Polym. Sci. **173**, 105 (2005).
34. J.S. Eow, M. Ghadiri, A. Sharif, Colloids Surf. A: Physicochem. Eng. Asp. **225**, 193 (2003).
35. J.S. Eow, M. Ghadiri, A. Sharif, J. Electrostat. **51**, 463 (2001).
36. W. Hong, X. Ye, R. Xue, J. Disper. Sci. Technol. **39**, 26 (2017).
37. Q. Yang, B. Li, H. Tian, X. Li, J. Shao, X. Chen, F. Xu, ACS Appl. Mater. Interfaces **8**, 17668 (2016).
38. J.D. Sherwood, J. Fluid Mech. **188**, 133 (1988).